Frequency-Domain Analysis and Design of Thomson-Coil Actuators

Bruno Lequesne
E-Motors Consulting, LLC
Menomonee Falls, WI, USA
bruno.lequesne@ieee.org

Tyler Holp
Circuit Protection Division
Eaton Corp.
Moon Twp, PA, USA
TylerHolp@eaton.com

Steve Schmalz
Eaton Research Labs
Eaton Corp.
Menomonee Falls, WI, USA
SteveSchmalz@eaton.com

Michael Slepian
Circuit Protection Division
Eaton Corp.
Moon Twp, PA, USA
MichaelSlepian@eaton.com

Hongbin Wang
Eaton Research Labs
Eaton Corp.
Menomonee Falls, WI, USA
HongbinWang@eaton.com

***Abstract*— Thomson coil actuators consist of an electric coil repelling a metallic disk. They are considered the fastest electromagnetic actuators for short travels and for this reason are favored for DC circuit breakers. Although the basic physics are understood, the actuator's few components are very interdependent, making for a difficult analysis. Actuator design so far has thus been limited to trial and error based on finite-element models. In this paper, a novel approach is presented based on the electromagnetic frequency response of the actuator. This method is shown to be an intriguing analysis tool and various actuator design directions are presented. Experimental results provide a confirmation of the analysis.**

Keywords—Actuator, circuit breaker, Thomson coil, DC breaker

I. INTRODUCTION

DC grids are enjoying a renaissance due to the development of renewable energy and the emergence of DC loads such as data centers. The interruption of current under fault is however an issue because unlike AC, the current does not naturally cross zero. Effective DC circuit breakers have thus been identified as key enablers for the future grid [1]. To provide fast interruption with minimal losses and at a reasonable price, hybrid configurations have been proposed: An electromechanical actuator breaks the circuit while the current is temporarily diverted [2]-[5]. Fast electromechanical actuation is needed though to minimize the stress on the semiconductors through which the fault current is diverted, and Thomson coils are prime candidates for this [5]-[21]. They are the focus of the paper.

A Thomson coil actuator is shown schematically in Fig. 1, along with the exciting circuit (Fig. 2). The actuator consists of a coil which when excited by a current pulse, induces eddy currents in the disk, thus repelling it. The current pulse is the result of the capacitor discharge following the switching on of the circuit thyristor (Fig. 2).

The basic operation of the actuator has been described before [6],[7]. Early authors developed the relevant mathematical derivations for Thomson-coil actuators, quite complex because of the transient aspect and geometrically diffuse nature of the induced currents [6],[7],[9]. The circuit itself is an LCR system, but one where the inductance varies with frequency and disk position. Due to this complexity, some researchers have used

The information, data, or work presented herein was funded in part by the U.S. Department of Energy Advanced Research Project Agency (ARPA-E), under Award Number DE-AR0001111.

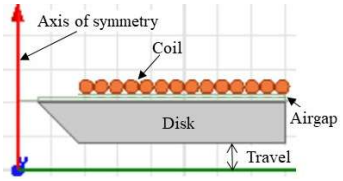

Fig. 1. Thomson-coil actuator model

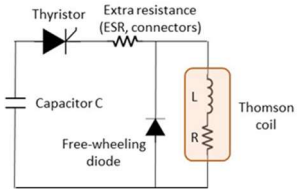

Fig. 2: Thomson-coil circuit

experimentation [8],[18]. More recently, designers have relied increasingly on finite element analysis (FEA) [9],[11],[15],[16], even multiphysics [121],[13],[17],[18],[20] the latter in order to include the mechanical aspect of the problem (such as to assess the stress and flexing of the moving disk [18]). Therefore, the basics physics are understood, and engineers have a tool to predict performance.

However, even with such powerful methods, design is still a challenge. The apparatus needs to be reasonably sized, along with energy, voltage, and current levels, leading to an optimization process aimed at getting the fastest motion with the smallest voltage, current, and size possible. While automated optimization is now available [22], a deeper understanding of the factors at play will facilitate reaching a satisfactory trade-off. To this end, this paper proposes a new approach based on the frequency response of the actuator. This approach provides new insights, including the finding of an electromechanical resonance, and makes it possible to reach a new understanding of design parameter interaction. This approach provides a physically sound view of the problem, as corroborated by tests and FEA, while making it possible to analyze design parameters independently of one another.

The paper is organized as follows. A first section describes the system in more details, presents the FEA analysis as well as experimental data for an early prototype. So validated, the FEA is used at various stages of the analysis to justify or corroborate simplifying hypotheses and partial results. Then, the new modeling approach is described. The method is finally used to analyze a number of actuator design parameters.

II. SYSTEM DESCRIPTION, TEST SETUP, AND FEA MODEL

A. System Description

The target application for the Thomson-coil actuator is a DC circuit breaker, shown schematically in Fig. 3 with the vacuum

interrupter on top, the Thomson-coil actuator below and a damping mechanism at the bottom. Motion is downwards. The selection and design of the vacuum interrupter and damping mechanism are beyond the scope of the paper.

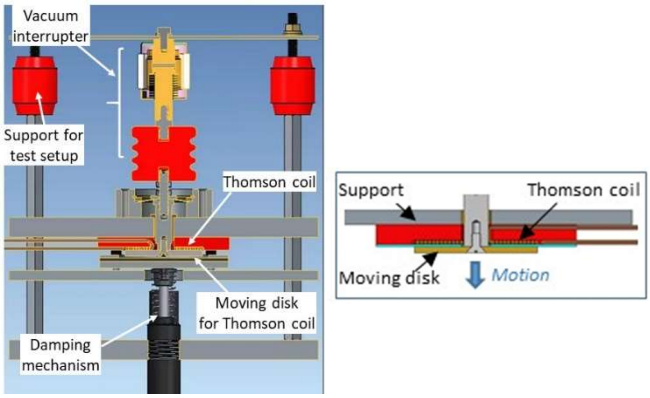

Fig. 3. Overall DC breaker system (left) and Thomson coil actuator (right)

The experimental setup is shown in Fig. 4. The dimensions for the actuator are given in Table I. This set-up was built early on to assess a number of factors concerning the actuator and other aspects of the system. As such, the design was a working tool not intended to be optimal. The moving mass, 500g, includes the moving parts of the vacuum interrupter, shaft, and damping mechanism. The disk was made of aluminum (alloy 6061-T6) which is mechanically stronger than copper, offsetting its higher resistivity in terms of overall performance [15],[18]. Motion was measured with a laser sensor. From a system perspective, ultimately, the target is for the breaker to open 6kV at 1kA peak with a peak allowable clamping voltage across the breaker of 12kV. The actuator itself will be designed to reach 1mm travel (out of a total 6mm) within 0.5ms [1].

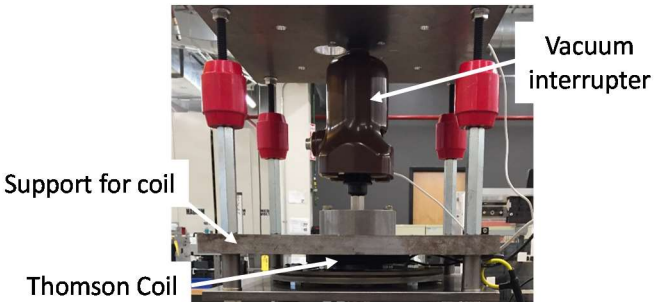

Fig. 4. Picture of the experimental setup

TABLE I. THOMSON-COIL ACTUATOR PROTOTYPE DIMENSIONS

Disk	Inner radius	3.2 mm
	Outer radius	38.1 mm
	Thickness	6.0 mm
	Material	Aluminum 6061-T6
Coil	Number of turns	14
	Wire size	12 AWG
	Inner radius	9.3 mm
	Outer radius	38.1 mm
Airgap	Length	0.8 mm
Load	Mass	500 g
Capacitor (electrolytic)	Capacitance	20 mF
	Voltage	275 V

B. FEA Model and Test Results

The FEA model used ANSYS Maxwell for the magnetic problem (Fig. 1), and Simplorer for the exciting circuit (Fig. 2). Thanks to axisymmetry, a 2D model takes full account of the geometry. Fig. 5 shows the correlation between FEA and tests, current (left) and position (right). Note that an extra resistance and inductance were added to the circuit (30mΩ and 3.0μH). These correspond to the circuit parasitic resistances and inductances, such as the capacitor ESR, wires, and connectors, which are significant given the low inductance (3 to 5μH) and resistance (around 12mΩ) of the coil. Such adjustments are common in this context [17]. No particular attention was given to minimizing parasitic elements at this early stage of the project. The current (up to and beyond peak value) is well modeled. Early displacement is also, although later position values are off, likely because of insufficient details concerning the mechanical load and system, including the 0.8mm airgap estimate. The tests used a damping mechanism for the end of motion, not included in the model which instead had a hard stop at 6mm. These encouraging test results make it possible to use the FEA analysis to verify the validity of various hypotheses and results of the new approach.

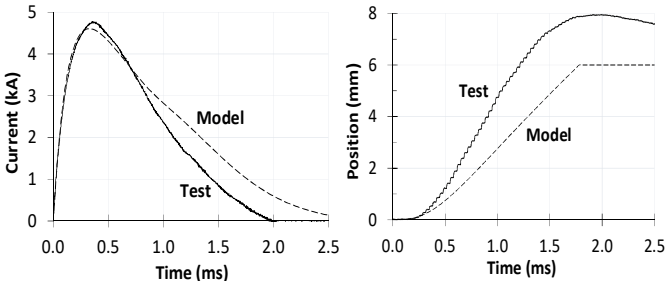

Fig. 5. Test and FEA results: Current (left) and displacement (right)

III. SYSTEM EQUATIONS

A. Circuit Equations

The coil drive is an RLC circuit (Fig. 2). The capacitor C holds the energy for the motion. The inductance L is the inductance of the coil (plus wires and capacitor). L varies with frequency and disk position. As will be seen later though, the range for L is relatively small (2 to 1 or so), so as a first step, it is assumed constant. The resistance R is the sum of the inner resistance of the capacitor (ESR), the resistance of the wires and connectors, and of the coil. It is also impacted by frequency, but only at frequencies beyond practical coil designs.

RLC circuit equations are well known. Specifically:

- The initial slope of current I versus time is voltage V over inductance L. Capacitance is not a factor:

$$\left(\frac{dI}{dt}\right)_{time=0} = \frac{V}{L} \quad (1)$$

- The current waveform is critically damped for the following value of R, and underdamped or overdamped if R is below or above this value, respectively:

$$R = 2\sqrt{L/C} \quad (2)$$

- The time for current peak, t_{peak}, is given by:

$$t_{peak} = \varphi / B \quad (3)$$

with, if underdamped: $\tan(\varphi) = \frac{B}{A}$

or if overdamped: $\tanh(\varphi) = \frac{B}{A}$

where: $A = \frac{R}{2L}$ and $B = \sqrt{\frac{|4L - R^2C|}{4L^2\,C}}$

- The maximum value of t_{peak} occurs when R=0:

$$t_{peak}\ (\max) = \frac{\pi}{2}\sqrt{LC} \tag{4}$$

which corresponds to the minimum frequency f_{min}:

$$f_{min} = \frac{1}{2\pi\sqrt{LC}} \tag{5}$$

The current therefore starts with the same slope V/L regardless of the resistance and capacitance values. However, the larger the resistance, the earlier and thus the lower the peak current. Minimizing the resistance, especially the capacitor ESR, is therefore a critical aspect of an effective design.

B. Impact of Motion on Current and Force Levels

Current generates force, and force is the source of motion. At the same time, motion has an impact on current and thus force, in three ways: First, a larger airgap reduces the coupling between coil and disk, thus lowering the force. Second, the reluctance of the flux generated by the coil changes with position. Third, there are motion-induced eddy currents. The latter are usually not considered [6],[7], but the case can be made that all three can be neglected, because force and current develop before much motion has occurred. Therefore, models without motion are sufficient to estimate current and force profiles.

To verify the validity of this assumption, the model was run with and without motion of the disk. The results are shown in Fig. 6. The current is hardly affected. The force profile is different, but only after the peak force has occurred. The force peaks early, before the current (noted also in [15],[17]). In other words, the change in inductance due to motion occurs late in the process, barely affecting current, force and therefore travel time.

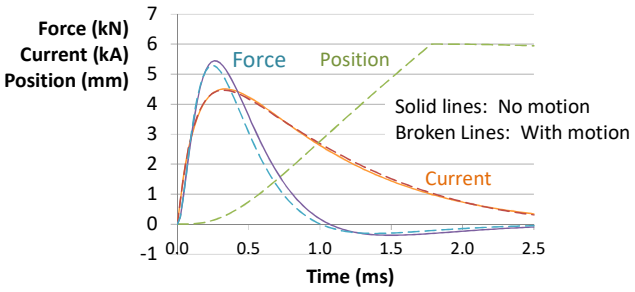

Fig. 6. Current and force, with and without motion (FEA)

C. Force on Thomson-Coil Disk

The repulsion force on the disk is the result of the interplay of the coil current with the current induced in the disk. A number of authors have derived it as a function of the coil current I_{coil}, disk current I_{disk} (induced by the coil current), and the mutual inductance M between the two, the latter in the form of its derivative with respect to displacement x (varying airgap) [10],[11],[19],[23],[24]:

$$F = I_{coil}\ I_{disk}\ \frac{dM}{dx} \tag{6}$$

For the present purpose, and as understood better later, it is useful to consider the case where the coil current is a sustained sinusoidal current:

$$I_{coil}\,(t) = I_{coil}\sin(\omega t) \tag{7}$$

A Thomson coil is essentially a transformer, with a single, short-circuited turn (the disk) as its secondary. Based on this analogy, if the coil current is sustained and sinusoidal, and with motion neglected, the induced current in the disk is also sinusoidal with a fundamental component at the same frequency and out of phase by some angle φ. Therefore:

$$I_{disk}\,(t) = I_{disk}\sin(\omega t + \varphi) \tag{8}$$

Again by analogy with transformers, the disk current is proportional to the coil current, by a factor k. k is the turns ratio between the secondary (1 with a solid disk) and the primary (number of coil turns), reduced by the presence of the airgap:

$$I_{disk} = k\,I_{coil} \tag{9}$$

Combining (6)-(9), we get the force F(t):

$$F(t) = k\,I_{coil}^2\sin(\omega t)\sin(\omega t + \varphi)\,\frac{dM}{dx} \tag{10}$$

After some manipulation, this force can be decomposed into a DC and an AC component:

$$F_{DC}(t) = \tfrac{1}{2}\,k\,I_{coil}^2\,\frac{dM}{dx}\,\cos(\varphi) \tag{11}$$

$$F_{AC}(t) = -\tfrac{1}{2}\,k\,I_{coil}^2\,\frac{dM}{dx}\,\cos(2\omega t + \varphi) \tag{12}$$

The following observations can be made: First, the force (both DC and AC components) is proportional to the square of the coil current magnitude. Second, the frequency of the AC force is twice that of the current (explaining why force peaks before current, Fig. 6). Further, the DC component is always smaller than the magnitude of the AC component, by the factor $\cos(\varphi)$, i.e. the phase lag between the disk and coil currents. Accordingly, under sustained excitation, the repulsion force will be negative once per period (this is the case in Fig. 6 after 1ms).

D. Circuit Pseudo Frequency and Travel Time

It was seen, Fig. 6, that the current and force peak early, and before the desired travel time (0.5ms). Said differently, if the current keeps flowing in the coil near the end of motion, or for that matter afterwards, such late currents and forces are useless (see also [15]). Stating thus that the current should peak at a time t_{ctpk} roughly equal to half the target time T_{tr}, one can derive an approximate target pseudo frequency f_{ps} for the coil current, since t_{ctpk} is 1/4th of the current period T_{ct}.

$$t_{ctpk} = \frac{T_{tr}}{2} \tag{13}$$

$$f_{ps} = \frac{1}{T_{ct}} = \frac{1}{4\,t_{ctpk}} = \frac{1}{2\,T_{tr}} \tag{14}$$

The pseudo frequency is related to circuit parameters L, C, and R by (3). This equation, however, does not lend itself to simple derivations. It is therefore convenient to relate the pseudo frequency of the circuit to its ideal frequency f_{LC} in the absence of resistance, with only L and C, given by (5). This ideal frequency will always be less than the circuit pseudo frequency. Assuming a factor of 2 (corroborated later in the paper, Section IV.B.2) yields, from (5):

$$f_{ps} = 2\, f_{LC} = \frac{1}{\pi\sqrt{LC}} \tag{15}$$

By combining (14) with (15), and noting that $\pi^2 \approx 10$, one gets a convenient target value for the product LC as a function of the desired target time:

$$L\,C = 0.4\; T_{tr}^2 \tag{16}$$

This formula appears better suited to the selection of the capacitance value than the capacitance energy ($E = \frac{1}{2} C\, V^2$) suggested at least indirectly by previous authors [15],[16].

IV. System Frequency Response : Approach , Results and Comparison with Transient Model

A. Approach and Results

As said in the introduction, previous authors have followed either one of two paths: Some developed the physical equations, in essence, they calculated the mutual inductance as a function of current and position, and developed the relationship "k" between disk and coil currents. Other solved these equations via FEA. It will be seen now that an alternative approach, based on a frequency analysis of the system, can provide useful insights, some never observed before. In short, it consists of replacing inherently transient equations with a stationary AC problem. This method will highlight the coupling between the electric circuit and the force, that is, between the electrical and mechanical systems.

To this effect, the FEA model of the prototype setup was run with an AC current of constant magnitude (an arbitrary 5kA) or voltage (250V) at frequencies from 0.1Hz to 1MHz. The resistance and inductance of the coil were derived as well as the force on the plate. The disk was stationary, as justified earlier.

Looking first at the circuit resistance, Fig. 7, it varies little until frequencies on the order of 5kHz, beyond the practical range for Thomson-coil actuators. The inductance (Fig. 8), on the other hand, is constant at low and high frequencies (8.5µH and 1µH, respectively), with a transition between 10Hz and 10kHz. At low frequencies, the flux penetrates deep in the disk, providing little reluctance to the flux. At high frequencies, the induced currents in the disk are strong and prevent the magnetic flux from extending beyond the airgap, making for a high reluctance. Comparing, finally, the resistance, reactance, and impedance of the circuit (Fig. 7), the coil is mostly resistive until around 1kHz, then largely inductive. As a result, for a constant voltage, the current is constant at low frequencies and drops to essentially zero at higher frequencies (Fig. 9).

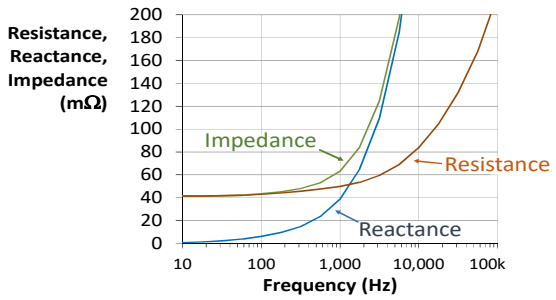

Fig. 7. Resistance, impedance and reactance vs. frequency

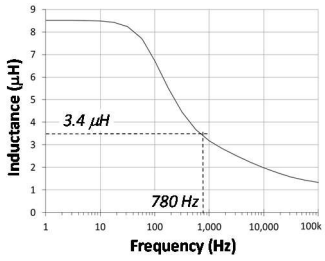

Fig. 8. Inductance vs. frequency

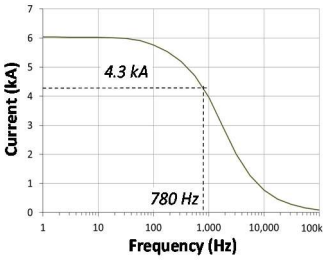

Fig. 9: Current vs. f. (constant voltage)

The most important result from this analysis, however, is the plot of AC and DC forces versus frequency for a constant voltage (Fig. 10.a) and constant current (Fig. 10.b). For a constant voltage, there is a clear resonance taking place in the electromechanical system, with a peak force occurring at a given frequency, around 400Hz in this case. At low frequencies, little current is induced in the disk, thus no force is produced. As frequency increases, so does the force. At high frequencies, the current in the coil is small due to the high circuit reactance. This drop in force occurs just below 1kHz, that is, the frequency at which the circuit goes from resistive to inductive (Fig. 7). If the reactance constraint is removed, the force keeps increasing, as shown in Fig. 10.b where force is calculated for a constant current. Note also that in both cases (constant voltage or current), the AC force is always equal or larger than the DC force, consistent with prior observations (11),(12). It is equal at both low and high frequencies, and larger during resonance.

Continuing on this analysis, Fig. 11 shows the phase of the AC force (phase lag relative to coil current) versus frequency, for a constant current. Based on (12), this is also the phase lag between disk and coil currents. It is similar to the phase shift between primary and secondary currents in a transformer, and goes from 0 to 90°. The transition, between 10Hz and 1kHz, matches the resonance of force at a constant voltage (Fig. 10.a).

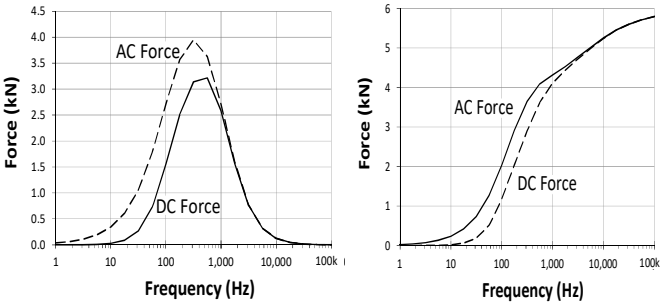

Fig. 10. Forces vs. frequency, with (a) constant voltage and (b) constant current

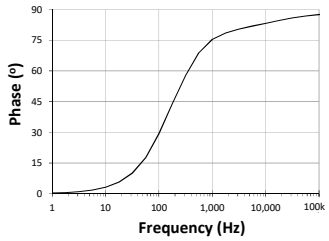

Fig. 11. Phase of AC force relative to coil current, vs. frequency

The conclusion is that there is a resonance within the electromechanical energy conversion, seen from the bell shape of the force profile. To the authors' knowledge, the existence of such a resonance in the actuator force has not been reported before in the literature. Further, it comes to reason that the force peak could be matched to advantage with the frequency of the electrical circuit. Another observation is that such an analysis could be used as a complement to the FEA model, in order to simplify the analysis of various design parameters. In the following section, the results of the frequency response analysis are compared with the more conventional transient model, to ensure that results from frequency analysis can quantitatively predict performance potential.

B. Comparing Frequency Response and Transient Model

1) Transient model: Fig. 12 shows the results of the transient model, as calculated by FEA for the same coil analyzed with frequency analysis, with the addition of motion. "Transient model" refers to the full FEA actuator model versus time, including disk motion, as opposed to the frequency analysis model. The data in Fig. 12 are the same as in Fig. 6, but with fewer traces and showing only the first 0.4ms, for clarity.

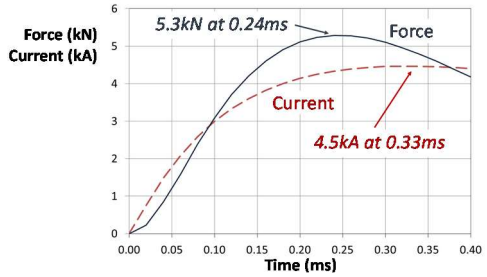

Fig. 12. Transient model: Force and current versus time for exemplary set-up

2) Pseudo frequency of the coil current: The first step in this comparison is to establish the circuit pseudo frequency from the frequency response. The pseudo frequency is given by (3), with L provided by the frequency response (Fig. 8). This must be solved by iteration, or graphically (Fig. 13). To do so, data for L are obtained for a range of frequencies, then the circuit operating pseudo frequency calculated, and the solution is when the pseudo frequency matches the input frequency: In Fig. 13, when the result crosses the y=x line.

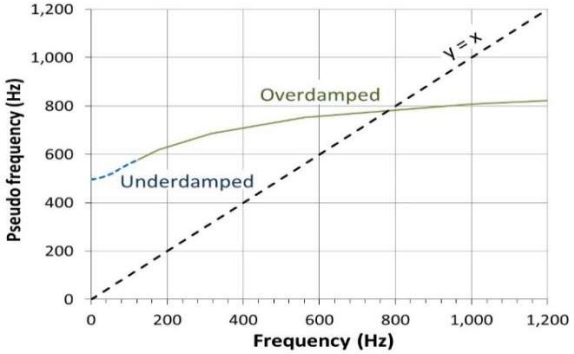

Fig. 13. Graphical solution of (3) for the prototype

In this instance, the circuit is underdamped until around 120Hz (broken trace), then overdamped. The solution is approximately 780Hz. At such a pseudo frequency, the current first peak occurs at 0.32ms. Referring back to Fig. 12, the transient model shows the current peaks at time 0.33ms, an excellent match. The frequency analysis (Fig. 13) assumes operation at a single frequency while the transient model takes into account the full complexity of the dependency of L and R on frequency. The closeness of the two results shows that it is adequate to assume that the system operates at a single frequency (or dominant frequency). Further, this value can be found by frequency analysis alone.

The pseudo frequency is also somewhat less than twice the frequency value when R=0, which can be similarly calculated to be 425Hz. This corroborates the selection of a factor of 2 leading to (15).

3) Current peak: The full transient model shows the current peaks at 4.5kA (Fig. 12). This value can be compared to the value obtained from the frequency response analysis, with the current graph shown as Fig. 9. At 780Hz, the current is around 4.3kA, very close to the 4.5kA found in the full model. This shows that a frequency response analysis is sufficient to predict both the peak value and timing of the current in the coil. Note that Fig. 9 was calculated for a constant voltage of 250V. The data in Fig. 12 are for a circuit energized by a capacitor with an initial voltage of 275V and a voltage reduced at time 0.32ms to 221V, such that 250V is a suitable average value.

4) Inductance: The inductance calculations with the two models can also be compared. The initial slope of current in an LCR circuit is V/L , where V is the initial capacitor voltage (1). The inductance can thus be calculated from Fig. 12 (transient model, initial voltage = 275V) as 6.65µH. With an extra circuit inductance of 3µH, this means the coil inductance is 3.35µH. Turning to the frequency analysis, the inductance is 3.4µH at 780Hz, see Fig. 8, a very close estimate.

5) Force: Fig. 12 also shows the force versus time. It peaks at time 0.24ms. It is logical to see it peak before the current, since the AC force oscillates at twice the frequency of the current (12). The peak value of the force is 5.3kN. This is, however, a transient value and a direct correlation with the frequency analysis is more difficult, since that analysis assumes steady-state sinusoidal excitation and calculates the DC and AC force separately. Referring to Fig. 10.a, the DC force around 780Hz is 2.9kN and the AC force magnitude is 3.1kN. The transient model result, 5.3kN, is more than the DC force alone (2.9kN), and less than the sum of both (6.0kN).

C. Circuit Pseudo Frequency and Force Resonance

It is important to consider at which frequency the force resonates. As seen in Fig. 10.a, the force peaks (resonates) around 500Hz (DC force) and 310Hz (AC force), below the circuit pseudo frequency (780Hz). If the system were operating at the force resonant frequency, the DC force would be 3.3kN

(14% more than at 780Hz) and the AC force magnitude would be 3.9kN (22% more than at 780Hz). It may thus be that this initial design was close to, but not at, optimum.

V. Actuator Parameter Analysis

A. Method

Frequency analysis makes it possible to analyze Thomson-coil actuators one parameter at a time, thus providing unique physical insights. This is done by analyzing geometries with FEA in Cartesian coordinates, where the disk, which now must be called plate, is infinitely long and very wide. In doing so, wire spacing, size, shape, airgap, material, coil size and a number of design parameters can be analyzed independently of one another. Figs. 14-15 illustrate this method for the case of wire spacing. The figures show the two wires and the large plate across the airgap, with current and flux densities at 60Hz. This geometry can easily be modeled by FEA to provide the frequency response of the system as a function of a single parameter, wire spacing in this example. Table II provides dimensions used for the analysis.

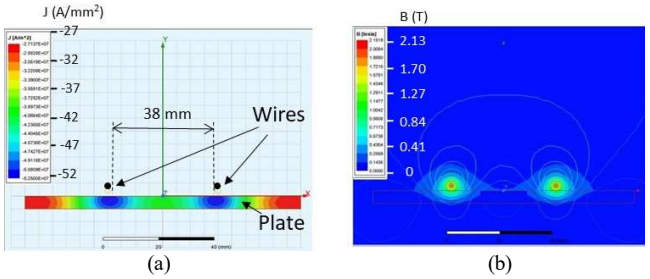

Fig. 14. Model of 2 wires, far apart; (a) Current densities; (b) Flux densities

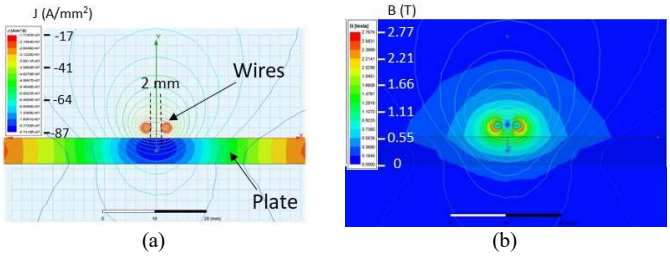

Fig. 15. Model of 2 wires, close together; (a) Current densities; (b) Flux densities (both Figs. 14 and 15 shown for 100V at 60Hz)

TABLE II. Dimensions for Thomson Coil Parameter Analysis

Plate	Width	200 mm
	Length	Infinite (2D)
	Thickness	5.0 mm
	Material	Copper
Wires	Diameter	2.0 mm
Airgap	Length	1.0 mm
Excitation	Voltage	100V

B. Wire Spacing

This answers the following questions: How far apart should the coil wires be from one another? How do neighboring coils interact with one another? This question is difficult to answer with a transient model of a given geometry, because a wider spacing means fewer turns, or smaller wires for a given coil diameter. For a practical geometry and with a transient model, wire spacing as a design parameter is inextricably linked to coil size, wire size, and turn number. The frequency response of such a system described in Figs. 14-15 is shown in Fig. 16, plotting the DC force only for clarity. The AC force was found to be consistently slightly more than the DC force, and peaking at about the same frequency (as shown in Fig. 10.a). Also shown in Fig. 16, in red, is the force from a single wire. When far apart, the two wires act independently and the total force is the sum of the forces from each wire. When very close, the total force is four times the force from one wire. Four is N^2, where N is the number of wires (N=2). When close, as illustrated in Fig. 17, there is a mutual inductance between each wire and the plate current induced not only by this wire, but by its neighbor as well. In this example, the transition occurs around 10mm. Therefore, adding to a coil width beyond this adds linearly to the force, whereas before that the growth is quadratic. Noting that what matters here is acceleration, not force, and since adding to the coil width requires adding to the moving disk mass, a diminished return may be reached.

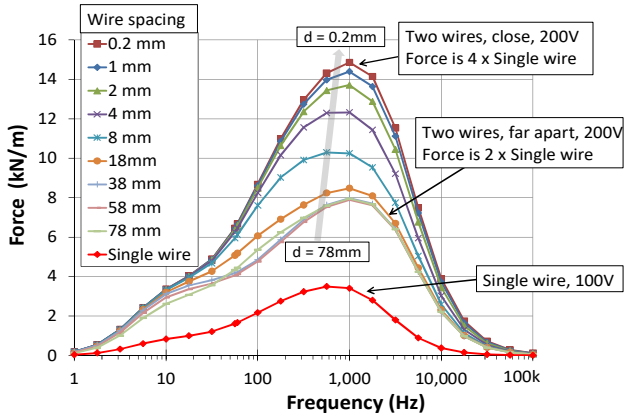

Fig. 16. Force pattern for various distances between 2 wires (constant voltage)

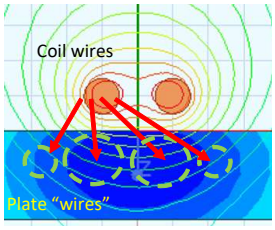

Fig. 17. Current induced by two wires and interaction with plate current (close-up of Fig. 15.a). The shades of blue indicate induced currents.

C. Coil Width

The coil width was analyzed by assuming a single, rectangular wire of thickness 1 mm at a 1-mm airgap from a large plate or disk. The problem was analyzed in both Cartesian coordinates and axisymmetric coordinates. Only the latter is shown for brevity. The results are qualitatively similar, the difference being that in the axisymmetric geometry when the coil width is increased, the length of the wire is also changed (longer) thus affecting the impedance of the coil. The model is

shown in Fig. 18 and the frequency response for a constant voltage in Fig. 19. Coil width was varied by keeping the inner radius constant (5mm) and changing the outer radius.

The force peak values can be fitted with respect to coil width by either one of two equations, one for smaller and the other for larger coil widths, For lower coil widths w, less than 10mm:

$$F_{peak} = \alpha w^2 e^{\lambda w} \qquad (\lambda = 0.11) \qquad (17)$$

and for larger widths (w > 10mm):

$$F_{peak} = \beta(w + \gamma)\,(1 - e^{\lambda w}) \qquad (\lambda = 0.20) \qquad (18)$$

where α, β and γ are constants selected for curve fitting.

The peaks of force versus frequency vary first as the square of the coil width (17), then proportionally after 10mm or so (18). This finding is consistent with the results concerning wire spacing. When the coil is wide, there is a diminishing return with wider coils due to the absence of mutual inductance between one end of the coil and the current induced by the other end of the coil. This diminishing return is amplified by the need for a larger disk thus mass with a wider coil.

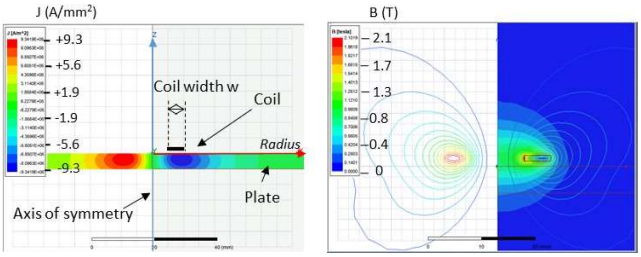

(a) (b)

Fig. 18. Model of coil width; (a) Current densities; (b) Flux densities (60Hz)

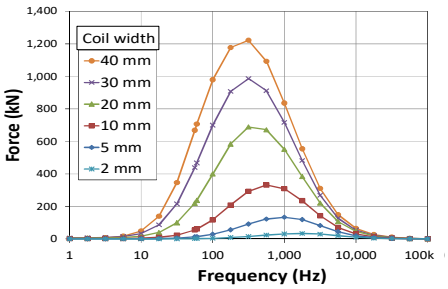

Fig. 19. Force pattern for various coil widths (Single wire at 100V)

D. Number of Turns for Given Coil Width

The selection of the number of turns is a critical design element. The difficulty, usually, consists of separating that question from a number of other ones, such as wire size, disk size, etc. To overcome this limitation, two similar problems, but with one important difference, are now compared. They are based on a given geometry with 16 turns facing a disk, connected as follows: In one case, all in series. In the other case, the turns are divided in two groups of 8, placed in parallel. In order to neutralize the effect of axisymmetry, whereby outer turns are longer than inner turns, the turns are assigned alternately to one group of 8 or the other from the inside to the outside of the coil. It follows that the parallel configuration, in essence, uses exactly half the number of equivalent turns, with everything else being the same.

The results are shown below, first force for a constant voltage (Fig. 20), then force for a constant line current (Fig. 21), which divides the current in half in each branch for the parallel case. The case with the 16 turns in series is shown on the left and the case of 8 turns in parallel with 8 other turns on the right. The results are direct ratios of one another. For a constant voltage, the force is 4 times larger with 8 turns in parallel with 8 others, because the current is twice as large and force goes with current square. For a constant overall line current, the opposite is true: The force is 4 times larger in the series case, because there are twice as many effective turns.

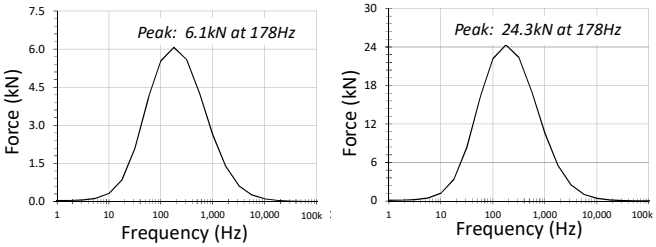

(a) (b)

Fig. 20. Force vs. frequency for constant voltage; (a) 16 turns in series; (b) 8 turns in parallel with 8 other turns

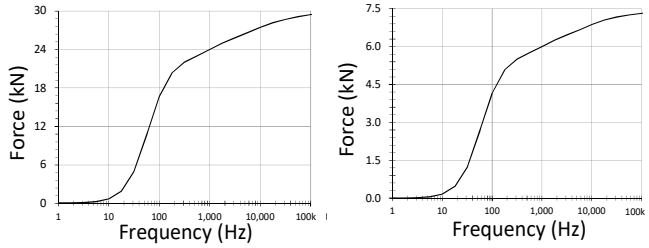

(a) (b)

Fig. 21. Force vs. frequency for constant current; (a) 16 turns in series; (b) 8 turns in parallel with 8 other turns

The conclusion is: If one operates within a current limit, it is better to have as many turns as possible, as this increases the Ampere-turns. Conversely, if there is a voltage limit, the fewer turns, the better, in order to draw as much current as possible. This is because the impedance of the circuit goes with N^2 (N being the number of turns equivalent), therefore for a given voltage, current goes with $1/N^2$ and the Ampere-turns (NI) go with 1/N. These principles can guide actuator design, with the thyristor rating establishing the current limit and the capacitor selection and charging circuit providing the voltage limit.

VI. Conclusions

The paper introduces a novel analysis technique for Thomson-coil actuators. It replaces the transient analysis used before either through complex equations or FEA, with a simpler analysis of the frequency response of the actuator. This perhaps counter-intuitive approach of replacing a transient problem with an analog stationary one was demonstrated to be valid, as predictions in terms of coil inductance, circuit pseudo-frequency, current magnitude and to some extent force level

were corroborated by FEA results, the FEA itself checked against experimental data.

Concerning Thomson-coil actuators, the new method made it possible to draw a number of general conclusions:

- The coil electric circuit operates at one dominant frequency, even though the inductance varies with frequency.
- The circuit operating frequency can be determined from frequency response analysis alone. It is also possible to calculate the peak current from frequency analysis, as well as an approximate value of force.
- The coil inductance and circuit capacitance are approximately related to the target travel time T_{tr} by:

$$L\,C = \ 0.4\ T_{tr}^2$$

- The force is a combination of a DC force and an AC force (when excited by a pure sinusoidal current). The frequency of the AC force is twice that of the current. The DC force is slightly less than the magnitude of the AC force, by $\cos\phi$, where ϕ is the phase shift between coil and disk currents.
- It was found that in Thomson-coil actuators, the force for a given voltage resonates at a given frequency. It would be desirable for this frequency to be also that of the coil circuit, or at least to be as close to it as possible.
- It is critical to reduce the circuit resistance as much as possible, especially the parasitic resistance, in order to have the largest current possible.
- Force depends on wire spacing to the square of the distance for small values, and linearly beyond. Similarly, coil width goes quadratically, then linearly as width increases.
- The number of turns should be selected to balance and maximize the thyristor current and capacitor voltage ratings: More turns for a given current, fewer turns for a given voltage.

More generally, the paper introduces a novel approach to the study of transients in electromechanical systems by replacing the transient problem with a simpler one involving the frequency response of the system, which the authors surmise may find useful applications beyond Thomson-coil actuators.

VII. Acknowledgements

The authors are grateful to Messrs. Mahesh Varrier and Arjun Tr of Eaton who provided the initial ANSYS Maxwell model, and to Mr. James Counihan of the Eaton Circuit Protection Division for his assistance with the tests.

VIII. References

[1] US Dept. of Energy, “Building Reliable Electronics to Achieve Kilovolt Effective Ratings Safely”, https://arpa-e.energy.gov/technologies/programs/breakers Retrieved May 05, 2021.

[2] J.-M. Meyer, A. Rufer, “A DC hybrid circuit breaker with ultra-fast contact opening and integrated gate-commutated thyristors (IGCTs)”, IEEE Trans. Power Delivery, Vol. 21, No. 2, 2006.

[3] W. Wen, Y. Huang, M. Al-Dweikat, Z. Zhang, T. Cheng, S. Gao, W. Liu, “Research on operating mechanism for ultra-fast 40.5 kV vacuum switches,” IEEE Trans. Power Delivery, Vol. 30, no. 6, 2015.

[4] C. Peng, X. Song, A.Q. Huang, I. Husain, "A medium-voltage hybrid DC circuit breaker—Part II: Ultrafast mechanical switch," IEEE Journal Emerg. Sel. Topics in Power Electron., vol. 5, no. 1, pp. 289-296, March 2017.

[5] C. Xu, T. Damle, L. Graber, "A Survey on mechanical switches for hybrid circuit breakers," 2019 IEEE Power & Energy Society General Meeting (PESGM), 2019, pp. 1-5.

[6] S. Basu, K.D. Srivastava, “Analysis of a fast acting circuit breaker mechanism, Part I : Electrical aspects”, IEEE Trans. Power Apparatus and Systems, Vol. PAS-91, No. 3, 1972.

[7] S. Basu, K.D. Srivastava, “Analysis of a fast acting circuit breaker mechanism, Part II : Thermal and mechanical aspects”, IEEE Trans. Power App. Systems, Vol. PAS-91, No. 3, 1972.

[8] R.J. Rajotte, M.G. Drouet, “Experimental analysis of a fast acting circuit breaker mechanism: Electrical aspects”, IEEE Trans. Power App. Systems, Vol. PAS-94, No. 1, 1975.

[9] T. Takeuchi, K. Koyama, M. Tsukima, “Electromagnetic analysis coupled with motion for high-speed circuit breakers of eddy current repulsion using the Tableau approach”, Electrical Engineering in Japan, Vol. 152, No. 4, 2005.

[10] B. Roodenburg, T. Huijser, B.H. Evenblij, "Simulation of an electro magnetic (EM) drive for a fast opening circuit breaker contact," 2005 IEE Pulsed Power Symposium, Basingstoke, UK, 2005.

[11] Z. Jian, J. Zhuang, C. Wang, J. Wu, L. Liu, "Simulation analysis and design of a high speed mechanical contact base on electro-magnetic repulsion mechanism," 2011 Intern. Conf. on Electrical Machines and Systems, Beijing, 2011.

[12] A. Bissal, J. Magnusson, E. Salinas, G. Engdahl, A. Eriksson, “On the design of ultra-fast electromechanical actuators: A comprehensive multi-physical simulation model”, 2012 Sixth Intern. Conf. on Electromagnetic Field Problems and Applications.

[13] A. Bissal, A. Eriksson, J. Magnusson, G. Engdahl, “Hybrid multi-physics modeling of an ultra-fast electro-mechanical actuator”, Actuators 2015, 4, pp. 314-335.

[14] V. Puumala, L. Kettunen, "Electromagnetic Design of Ultrafast Electromechanical Switches," IEEE Trans. Power Delivery, vol. 30, no. 3, June 2015.

[15] A. Bissal, J. Magnusson, G. Engdahl, “Electric to mechanical energy conversion of linear ultrafast electromechanical actuators based on stroke requirements”, IEEE Trans. Indus. Appl., Vol. 51, No. 4, July/Aug. 2015.

[16] D.S. Vilchis-Rodriguez, R. Shuttleworth, M. Barnes, "Finite element analysis and efficiency improvement of the Thomson coil actuator," 8th IET Intern. Conf. Power Electronics, Machines and Drives, 2016.

[17] C. Peng, I. Husain, A. Huang, B. Lequesne, R. Briggs, “A fast mechanical switch for medium voltage hybrid DC and AC circuit breakers,” IEEE Trans. Indus. Appl., Vol. 52, No. 4, July/Aug 2016.

[18] C. Peng, “Design, optimization and development of ultra-fast mechanical switch for DC circuit breaker applications,” PhD dissertation, EE Dept., Noth Carolina State University, Raleigh, North Carolina, 2016.

[19] D.S. Vilchis-Rodriguez, R. Shuttleworth, M. Barnes, "Modelling Thomson coils with axis-symmetric problems: Practical accuracy considerations," IEEE Trans. Energy Convers., vol. 32, no. 2, pp. 629-639, June 2017.

[20] A. Baudoin, B. Hátsági, M. Álvarez, L. Ängquist, S. Nee, S. Norrga, T. Modeer, “Experimental results from a Thomson-coil actuator for a vacuum interrupter in an HVDC breaker”, The Journal of Engineering, Vol. 2019, No. 17, 2019 (IET).

[21] C. Xu, T. Damle, L. Graber, "A survey on mechanical switches for hybrid circuit breakers," 2019 IEEE Power & Energy Society General Meeting (PESGM), 2019, pp. 1-5.

[22] G.Y. Sizov, P. Zhang, D.M. Ionel, N.A.O. Demerdash. M. Rosu, "Automated multi-objective design optimization of PM AC machines using computationally efficient FEA and differential evolution," IEEE Trans. Indus. Appl., vol. 49, no. 5, pp. 2086-2096, Sept.-Oct. 2013.

[23] G.R. Slemon, “*Magnetoelectric Devices: Transducers, Transformers and Machines*”, John Wiley & Sons, New York, 1966.

[24] M.A. Juds, “Thomson Coil”, in *Practical Magnetic and Electomechanical Design – Solenoids, Actuators, Transformers, Inductors*, bookbaby.com, 2020, ch. 14, pp. 211-227.